Structural and Thermodynamic Properties of Electrolyte Solutions in Hard-Sphere Confinement: Predictions of the Replica Integral Equation Theory

Barbara Hribar,[†,‡] Vojko Vlachy,*[,†] and Orest Pizio[‡]

Faculty of Chemistry and Chemical Technology, University of Ljubljana, Ljubljana 1001, Slovenia Instituto de Química de la UNAM, Circuito Exterior, Coyoacán 04510, México, D.F.

Received: December 9, 1999

The structural and thermodynamic properties of the primitive model for 1−1, 2−1, 3−1, and 4−1 electrolyte solutions in a disordered hard sphere matrix environment mimicking a microporous adsorbent were studied. The size of the matrix species and the matrix density were chosen as in the model of silica xerogel proposed by Kaminsky and Monson. The majority of the results of our study follows from the application of the replica Ornstein−Zernike (ROZ) integral equations complemented by the hypernetted-chain (HNC) closure. Theoretical predictions were tested versus Monte Carlo computer simulation results for one of the most difficult cases studied here, i.e., for a charge and size asymmetric 3−1 electrolyte, with the parameters mimicking $LaCl_3$ solution. Steric effects due to matrix confinement are seen to influence substantially the equilibrium properties of the annealed electrolyte. In particular, our results show the development of a net attraction between the like-charged ions at small separations, not present in the absence of matrix. The pair distribution functions and thermodynamic properties of 3−1 electrolytes confined by the matrix were compared with data for pure electrolyte and with the results for a mixture of 3−1 electrolyte with a fully mobile neutral component. The excess chemical potential for adsorbed electrolyte in a dense uncharged matrix is close to that of the fully annealed mixture of the electrolyte and matrix species under the same conditions. We attribute this result to a large difference in size between the matrix and electrolyte particles, i.e., to low mobility of matrix particles versus the ions in the mixture. The comparison between Monte Carlo results and the replica integral equation theory for a 3−1 model electrolyte indicates the theory is successful: the ROZ/HNC approach provides reasonably accurate predictions for structural and thermodynamic properties.

1. Introduction

Recently there has been a growing interest in extending the methods of statistical thermodynamics to fluids confined in microporous materials. In general, the influence of three types of confinement on fluids has been examined. The first case involves micropores of highly idealized geometries; for example, cylindrical capillaries or planar slits (see refs 1 and 2 for a comprehensive review of the theoretical approaches and computer simulation methodology, respectively). The second type of confinement includes adsorbents of more complicated structure where the microporous material is considered as a disordered set of obstacles; see, e.g., ref 3. Adsorption of fluids in these types of microporous media is now receiving considerable theoretical attention, and some particular aspects of this problem actually represent the subject of the present study. However, in both aforementioned cases the adsorbent particles do not respond to the addition of an adsorbing fluid. In the third, related, yet different example, the effect of steric forces enters through addition of neutral macroparticles to the original solution. In the latter case,[4] one actually deals with a multicomponent mixture and the standard thermodynamic relations apply.

Theoretical methods for the description of the adsorption of fluids in disordered microporous adsorbents are considerably less developed than the methods which apply either to regular mixtures or to pores with an idealized geometry. Evaluation of the equilibrium properties of a fluid distributed inside a disordered microporous matrix involves taking a double average: first over the configurational states of the annealed fluid and then over the quenched degrees of freedom of the matrix. Computer simulations of these systems are obviously time-consuming, since the usual canonical averages for the fluid structure must be obtained for a set of realizations of the matrix medium.[5−7]

The pioneering studies of Madden and Glandt,[8] Given and Stell,[9−11] and subsequent developments by other authors[12−14] (see refs 3 and 15 for reviews), have provided the theoretical methods to calculate the properties of quenched-annealed systems using techniques from liquid-state statistical mechanics. The application of the replica method has led to a formulation of the so-called replica Ornstein−Zernike (ROZ) equations and the appropriate closure relations. In addition, questions concerning the thermodynamics of these systems have been addressed within the continuum replica formalism.[12−14,16] In all the aforementioned studies systems with short-range forces were studied.

More recently, studies of partly quenched systems with Coulomb interactions have been undertaken.[7,17−20] The Debye−Hückel type of approach has been implemented by Chandler, Bratko, and Chakraborty in refs 7 and 17. On the other hand, Hribar et al.[21−23] obtained the screened potentials for pointlike partly quenched ionic fluids and successfully applied the ROZ theory in the mean-spherical approximation (MSA) and the hypernetted-chain (HNC) approximation to the restricted primi-

[†] University of Ljubljana.
[‡] Instituto de Química de la UNAM.

10.1021/jp994324p CCC: $19.00
Published on Web 04/13/2000

tive model of electrolyte solutions in a disordered medium of charged obstacles.

The principal concern of this paper is application of the ROZ theory to predict the structural and thermodynamic properties of a wide set of primitive model electrolyte solutions adsorbed in a hard-sphere matrix. The ROZ approach has not yet been implemented for this type of system. The motivation for the present study is manifold. First we wished to perform a test of the replica-type HNC closure for the model in question. Therefore, in addition to the ROZ/HNC calculations, we performed computer simulations for one of the most strongly interacting cases, i.e., for a 3−1 electrolyte modeling $LiCl_3$ solutions. The results obtained in this work may seemingly be extended to understand the effective interactions between macroions in systems with a larger charge and size asymmetry between the ions than considered in this study. Further, we considered that the knowledge about the structure and thermodynamics of the adsorbed electrolyte arising from this study could be helpful in developing a theory for phase transition. The theory could possibly be developed along the lines proposed by Kierlik et al.[13] In addition, the algorithms applied in the present work may be of considerable help in future extensions of the model.

In the present study our attention was focused on electrolytes in a dense confinement. The matrix was chosen to correspond to an equilibrium configuration of hard spheres: the size of matrix particles and the matrix density were chosen to be similar to the model used by Kaminsky and Monson (KM)[5] to describe the adsorption of methane in silica xerogel. However, to elucidate clearly the effects of the excluded-volume, we have not included any fluid−matrix attraction in our model, in contrast to the original KM model.[5] As in previous studies,[22,23] the replica OZ integral equation, complemented by the HNC approximation, was used to obtain the pair correlation functions for ion−ion and ion−matrix distribution functions. The HNC approximation belongs to the class of approximate closures that, in contrast to the Percus−Yevick or the mean-spherical approximation, take into account the so-called blocking effects of a disordered matrix medium. The blocking contributions to the correlation functions for ions confined by hard-sphere matrices to our knowledge have not been discussed in the literature so far.

The thermodynamic properties of electrolytes under strong confinement are clearly of major interest. In this paper the excess internal energy and the compressibility of the adsorbed electrolytes were calculated using the well-established routes used previously for uncharged partly quenched fluids.[9−11] Perhaps the most interesting quantity examined here is the excess chemical potential of the adsorbed electrolyte. The chemical potentials of various ionic species determine the equilibrium between the bulk solution and the confined electrolyte. So far, no suitable general equation for the chemical potential of adsorbed species (see ref 16 for a discussion of chemical potential in partly quenched fluids) has been proposed. In this paper, we extended the OZ/HNC expression for the chemical potential valid for bulk fluids[24,25] to the case of the partly quenched systems in question. The new expression, valid within the ROZ/HNC formalism, was tested against our simulation results for the excess chemical potential. In addition, thermodynamic and structural properties of the annealed 3−1 electrolyte in the matrix were compared with (a) the corresponding properties of the bulk 3−1 electrolyte and (b) with the results for the mixture of charged and uncharged species, where all components are free to equilibrate in the mixture and are therefore treated on an equal level. It has been shown before[6] that for a large size ratio between the matrix and the adsorbed fluid particles, the properties of the annealed fluid in a partly quenched system are close to those of a regular mixture consisting of matrix and fluid particles. We intended to clarify whether the same similarity between the partly quenched systems and regular mixtures exists for electrolytes adsorbed in a hard-sphere matrix.

2. Model Systems

The systems under study consist of two components. The quenched component is called the matrix and is represented by a one-component hard-sphere fluid. The second component is an annealed ionic fluid which equilibrates in the presence of matrix species. The notation of this paper is similar to that in refs 9−11 and 21−23: the superscripts or subscripts 0 and 1 correspond to the matrix and the annealed fluid species, respectively. The interaction potential between the matrix particles is

$$U_{ij}^{00}(r) = \begin{cases} \infty, & r < \sigma_0 \\ 0, & r \geq \sigma_0 \end{cases} \tag{1}$$

where σ_0 is the hard-sphere diameter. We restrict ourselves to the case where $\sigma_0 = 26.93$ Å and to the matrix packing fraction $\eta_0 = 0.3956$; i.e., the matrix species concentration is $c_0 = 0.06$ mol/dm^3. The microporosity of the matrix can formally be defined as $1 - \eta_0$.

In analogy with previous studies,[9−13,26] we assume that the matrix structure corresponds to an equilibrium state of the hard-sphere fluid. Then, the matrix structure can be sufficiently well approximated by the correlation function following from the solution of the Ornstein−Zernike equation with the Percus−Yevick (PY) closure. The ion−matrix interaction potential is assumed to be additive:

$$U_{i0}^{10}(r) = \begin{cases} \infty, & r < (\sigma_i^1 + \sigma_0)/2 \\ 0, & r \geq (\sigma_i^1 + \sigma_0)/2 \end{cases} \tag{2}$$

where σ_i is the diameter of an ion of species i. The electrolyte solution (annealed component) is considered within the primitive model, i.e., only the interactions between ions are taken into account explicitly, whereas the solvent is considered to be a continuous dielectric. The ion−ion potential reads

$$U_{ij}^{11}(r) = \begin{cases} \infty, & r < (\sigma_i^1 + \sigma_j^1)/2 \\ e^2 z_i^1 z_j^1/\epsilon r, & r \geq (\sigma_i^1 + \sigma_j^1)/2 \end{cases} \tag{3}$$

where ϵ is the dielectric constant of the continuum representing the solvent, which has the value of pure water at a given temperature. Several different electrolyte solutions whose parameters were chosen to model NaCl, LiCl, $CaCl_2$, $LaCl_3$, and $ThCl_4$ were studied at $T_1 = 298.15$ K. As suggested in a recent study of Simonin et al.,[27] we chose the diameter of a chlorine anion as $\sigma_{Cl} = 3.62$ Å, while the diameters of cations were $\sigma_{Na} = 3.87$ Å, $\sigma_{Li} = 5.43$ Å, $\sigma_{Ca} = 7.03$ Å, $\sigma_{La} = 7.75$ Å, and $\sigma_{Th} = 12.1$ Å. This choice of parameters permited us to get an insight into the interplay of the effects of size and charge of various ions composing the electrolyte, all studied for the same matrix medium.

3. Theoretical Methods

As mentioned in the Introduction, the majority of the results were calculated using the ROZ theory with the HNC closure.

On the other hand, to get some information about the accuracy of the ROZ/HNC theory, we performed computer simulations for a limited number of examples. The simulation results were obtained by the canonical Monte Carlo (NVT) methodology. Alternatively, the simulations could have been performed in the grand canonical ensemble formalism; however, the latter method is less suitable for the dense system studied here.

Replica Ornstein−Zernike Equations. First we discuss briefly the ROZ equations. The matrix structure was obtained in terms of the pair correlation function h^{00}, following from the regular Ornstein−Zernike equation for a one-component fluid

$$h^{00} - c^{00} = c^{00} \otimes \rho^0 h^{00} \tag{4}$$

where the symbol ⊗ denotes convolution and r-dependencies here and below are omitted for the sake of brevity. The OZ equation was complemented by the PY closure

$$c^{00} = [\exp(-\beta U^{00}) - 1]\{1 + h^{00} - c^{00}\} \tag{5}$$

The ROZ equations for the fluid−matrix and fluid−fluid correlations read[9−11,21−23]

$$h_{i0}^{10} - c_{i0}^{10} = c_{i0}^{10} \otimes \rho^0 h^{00} + c_{ii}^{11} \otimes \rho_i^1 h_{i0}^{10} + c_{ij}^{11} \otimes \rho_j^1 h_{j0}^{10} - c_{ii}^{12} \otimes \rho_i^1 h_{i0}^{10} - c_{ij}^{12} \otimes \rho_j^1 h_{j0}^{10}$$

$$h_{ij}^{11} - c_{ij}^{11} = c_{i0}^{10} \otimes \rho^0 h_{0j}^{01} + c_{ii}^{11} \otimes \rho_i^1 h_{ij}^{11} + c_{ij}^{11} \otimes \rho_j^1 h_{jj}^{11} - c_{ii}^{12} \otimes \rho_i^1 h_{ij}^{21} - c_{ij}^{12} \otimes \rho_j^1 h_{jj}^{21}$$

$$h_{ij}^{12} - c_{ij}^{12} = c_{i0}^{10} \otimes \rho^0 h_{0j}^{01} + c_{ii}^{11} \otimes \rho_i^1 h_{ij}^{12} + c_{ij}^{11} \otimes \rho_j^1 h_{jj}^{12} + c_{ii}^{12} \otimes \rho_i^1 h_{ij}^{11} + c_{ij}^{12} \otimes \rho_j^1 h_{jj}^{11} - 2c_{ii}^{12} \otimes \rho_i^1 h_{ij}^{21} - 2c_{ij}^{12} \otimes \rho_j^1 h_{jj}^{21}, \tag{6}$$

where, i and j stand for + and −, respectively. The correlation functions h_{ij} and c_{ij} consist of connected and blocking parts (see, e.g., refs 9−11). Connected parts correspond to the correlations between particles within the same replica, whereas the blocking parts describe correlations between the particles from different replicas. The particles belonging to different replicas correlate via the matrix particles; however, they do not interact among themselves. The functions h^{12} and c^{12} represent the blocking contribution to the pair correlation functions and to the direct correlation functions of the annealed fluid (fluid−fluid functions) h^{11} and c^{11}, respectively.

In the present calculation, the ROZ equations were supplemented by the hypernetted chain closure in the form[22,23]

$$c^{mn} = \exp[-\beta U^{mn} + \gamma^{mn}] - 1 - \gamma^{mn}$$
$$c^{12} = \exp[\gamma^{12}] - 1 - \gamma^{12} \tag{7}$$

where $\gamma^{mn} = h^{mn} - c^{mn}$, and the superscripts m and n take values 0 and 1.

It is well-known that the Coulomb part of the interaction potential requires special treatment. The renormalization procedure for the Coulomb interaction must be applied first, before the set of eqs 6 and 7 can be solved numerically. According to this procedure, the fluid−fluid correlation functions are separated into short-range (s) and long-range contributions:[21−23]

$$c^{mm}(r) = c_{(s)}^{mm}(r) + \phi^{mm}(r)$$
$$c^{12}(r) = c_{(s)}^{12}(r) \tag{8}$$

and

$$h^{mn}(r) = h_{(s)}^{mn}(r) + q^{mn}(r) \tag{9}$$

where the superscripts m and n assume the values 1 and 2. Further, $c^{22}(r) = c^{11}(r)$, $c^{01}(r) = c^{02}(r)$, and $c^{22}(r) = c^{11}(r)$; $\phi^{22}(r) = \phi^{11}(r)$. Considering that the particles belonging to different replicas do not interact, we put $\phi^{12}(r) = 0$. By choosing the ϕ functions in the form of the Coulomb potential, we obtain the q functions as given in ref 22, except that $q^{10} = 0$. Due to the fact that matrix species are uncharged, the q^{12} functions also vanish. In other words, the Coulomb interactions cannot be mediated by neutral particles within the dielectric continuum model. As a result, the q^{11} functions assume the Debye−Hückel form:

$$q_{ij}^{11}(r) = -L_B z_i^1 z_j^1 \exp(-\kappa_1 r)/r \tag{10}$$

where $\kappa_1 = (4\pi\Sigma\rho_i^1(z_i^1)^2 L_B)^{1/2}$, $L_B = e^2/k_B\epsilon T_1 = 7.15$ Å at 298.15 K, and ρ_i^1 is the number concentration of the ionic species i. As usual, k_B denotes Boltzmann's constant.

The ROZ/HNC equations were solved numerically by direct iterations. In all the calculations the number of integration points was $N = 8192$ and the integration step $\Delta r = 0.05$ Å. By this choice we assured that even at low electrolyte concentration, and for the highest charge asymmetry in question, i.e., for 4−1 electrolytes, the pair correlation functions of ions approach unity at large distances. The iteration was relatively fast up to intermediate concentrations. However, for 3−1 and 4−1 electrolytes it became more and more difficult to obtain a convergent solution as the concentration of electrolyte was increased. For example, several hundred thousands of iterations were needed to obtain the structure for $ThCl_4$ at 0.275 mol/dm^3. These problems with convergence reflect difficulties in accommodating a rather concentrated electrolyte solutions in the very dense matrix. Application of a more sophisticated algorithm does not help in this respect. The highest concentration reached for each electrolyte model, however, was sufficient to observe the dominant role of the excluded-volume effects in shaping the structural and thermodynamic properties of adsorbed solutions.

Monte Carlo Simulations. The computer simulation of a quenched-annealed system involves a double average. The configurational properties of an adsorbed fluid were first averaged over the annealed degrees of freedom (for a chosen matrix configuration), and then averaged over the matrix configurations. Theoretically, the second average extends over all possible configurational states of a matrix, but in practice, a small number of equilibrium matrix realizations seems to be sufficient for several systems.[4]

As a first step in this part of the calculation we used the canonical Monte Carlo method to simulate the matrix, i.e., a hard-sphere fluid. The number of matrix particles, N_0, used in the simulations was 600, except for the lowest electrolyte concentration where it was 6×10^3. The matrix subsystem was equilibrated over 2×10^7 attempted configurations. The number of ions to be distributed within the equilibrium realization of the matrix was calculated according to the electrolyte concentration, and it varied from 400 (at low concentration) to 4×10^3 (at high concentration). To avoid effects due to the finite number of particles included in the simulation cell (only when an electrolyte was present), the Ewald summation method was used.[28] The ions, distributed within the quenched hard-sphere fluid representing the matrix were first equilibrated over the $(5-10) \times 10^6$ states. After the equilibration run, a production

run of $(3-5) \times 10^7$ attempted configurations was needed to obtain reasonable canonical averages for the annealed electrolyte.

A new simulation cycle was started by changing the equilibrium distribution of the quenched fluid (no ions were present during this part of the procedure) by running an additional 9×10^6 configurations. The final configuration was chosen as the next representative distribution of matrix particles. Then the ions were distributed in the system again and, with the matrix particles fixed in their positions, the averaging process for the annealed electrolyte was repeated.

This kind of simulation is obviously time-consuming, and not very many different matrix configurations could be explored during the simulation. In the preliminary stage of this study we investigated the influence of the number of matrix configurations used in the averaging process. The canonical averages over the configurational states of the annealed electrolyte appeared to differ very little from one equilibrium matrix realization to another. We explain this finding by the fact that we used a relatively large matrix subsystem (i.e., the number of matrix particles) in the simulation and due to the short-range nature of the correlation between the matrix particles and ions. For a sufficiently large system, i.e., for a macroscopic sample of matrix material, the adsorbed electrolyte would necessarily visit all the domains representing relevant distributions of the matrix particles. This kind of physical argument was presented by Wu, Hui, and Chandler[29] and by Chakraborty, Bratko and Chandler (see ref 26 of ref 18) in the discussion of equivalency between the quenched and the adiabatic annealed averages for large, self-averaging systems. Accordingly, only a few realizations of the matrix (two or three in most cases) were used for averaging over the possible matrix−particle distributions. In the course of simulation, we calculated the ion−ion and ion−matrix pair correlation functions, the excess internal energy of the system, and the individual chemical potentials of ions. The latter were obtained by using the Widom test particle insertion technique with the charge rescaling scheme.[30]

4. Results and Discussion

We begin the presentation of results with a discussion of structural properties.

Pair Distribution Functions (pdf's). First the results for 1−1 electrolytes in the disordered hard-sphere matrix are discussed. We studied two different models for 1−1 electrolytes, the first one mimicking NaCl solutions (in this case the diameters of cations and anions are almost equal), while in the second model, i.e., in LiCl solution, the cation is substantially larger than the anion. Both solutions were studied in the concentration range from 0.01 to 1.0 mol/dm^3. The evolution of the pdf's for the aforementioned 1−1 electrolytes with increasing electrolyte concentration is shown in Figures 1 and 2. In the case of NaCl solution only the function for cations, $g_{++}(r)$, is presented (Figure 1a). The pdf's for anions $g_{--}(r)$ and cations $g_{++}(r)$, namely, practically coincide due to the approximate equality of the diameters of these ions. As expected, the range of correlations between ions decreases with increasing electrolyte concentration. This behavior reflects the higher screening of the electrostatic forces and the increasing importance of the excluded-volume effect. The probability of finding equally charged ions at small separations increases with increasing electrolyte concentration. The shape of the function $g_{++}(r)$ (Figures 1a and 2a) and the small shoulder on the $g_{+-}(r)$ curve (see Figure 2b, solid line) demonstrate the existence of the like-charge (+ +) pairs and triplets (− + −) in the confined system.

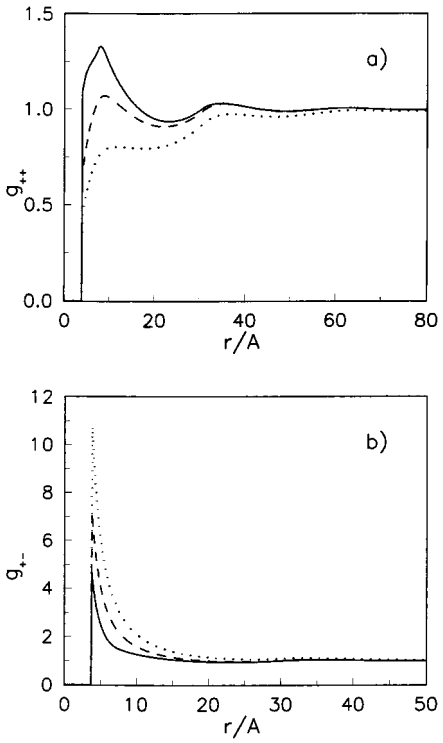

Figure 1. Pair distribution functions for (a) like-charged (+ +) ions and (b) oppositely charged ions for a model NaCl solution at concentrations (i) 0.01 mol/dm^3 (dotted line), (ii) 0.1 mol/dm^3 (dashed line), and (iii) 1.0 mol/dm^3 (solid line).

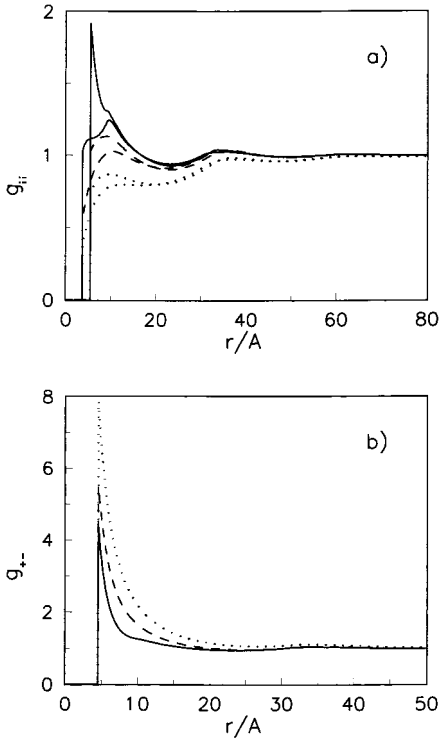

Figure 2. Same as Figure 1 but for a model LiCl solution. Legend as for Figure 1; the upper curves in part a correspond to + + and the lower curves to − − functions.

On the other hand, the small maximum at a larger distance in the function for the like-charge ions shows an increased probability of finding equally charged ions separated by a matrix particle. Our calculation therefore demonstrates that distribution functions for the adsorbed electrolyte phase differ from those of the corresponding bulk electrolyte which are either monoto-

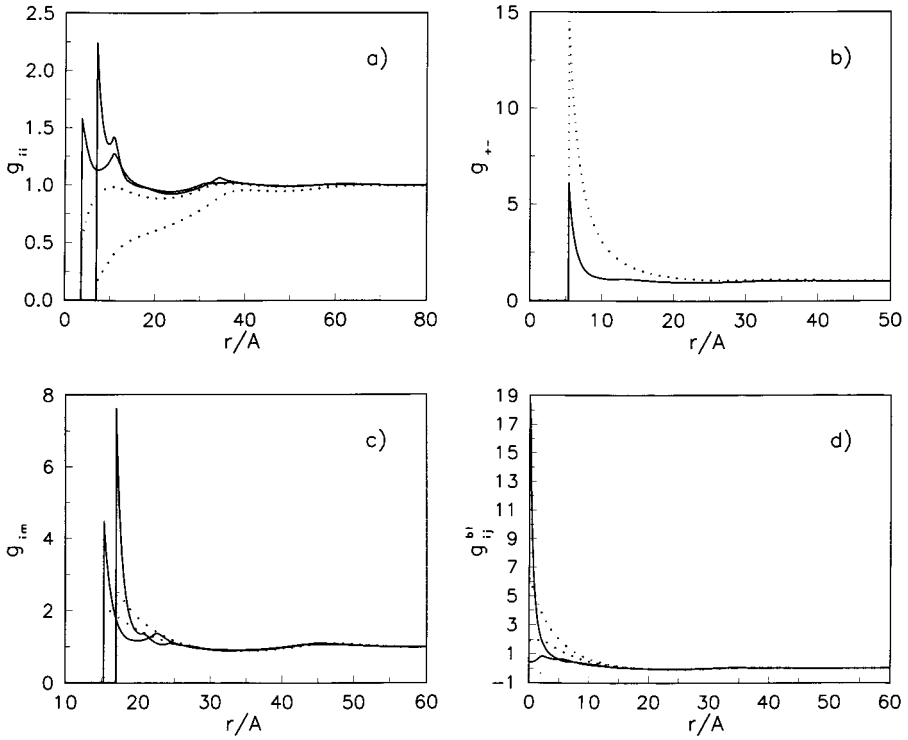

Figure 3. The pdf's for (a) like-charged ions, (b) oppositely charged ions, and (c) ion−matrix distributions all for a model $CaCl_2$ solution at concentration (i) 0.01 mol/dm^3 (dotted lines) and (ii) 0.9 mol/dm^3 (solid lines). In part d we present the blocking pdf's for $+ +$ and $+ -$ pairs. The solid and the dotted lines with a higher value at $r = 0$ are for $+ +$ pairs.

nously decreasing (for $+ -$ pairs) or increasing ($+ +$ and $- -$ pairs) functions of distance in this concentration range. The ion−matrix structure does not show any unusual features for 1−1 electrolytes, and we therefore proceed to a more interesting case, namely to the 2−1 electrolyte solution.

The pair-distribution functions for equally charged ions in the 2−1 electrolyte modeling a $CaCl_2$ solution exhibit a long-range repulsion (Figure 3a) at low concentrations; as expected, the doubly charged cations repel each other strongly. However, at higher concentrations there is a high probability for finding two equally charged ions in close proximity. Actually, the behavior observed previously for the LiCl model solution seems to be enhanced; cf. Figures 2a and 3a. On the other hand, there is a drastic decrease in the correlation range for oppositely charged ions with increase of electrolyte concentration (Figure 3b). While the correlations between the $+ -$ ions at small separations remain unaffected, the long-range asymptotic behavior is strongly suppressed. The evolution of the ion−matrix correlations with electrolyte concentration is shown in Figure 3c. The diameter of an ion influences the probability of finding that ion in contact with a matrix particle. For example, the Ca ion will be more likely in contact with a matrix particle than a smaller Cl ion. The distribution functions shown in Figure 3c demonstrate the presence of a layered structure, with ions of alternating charge on the surface of a matrix particle. This conclusion follows from the positions of the maxima in the ion−matrix pair-distribution function, $g_{im}(r)$, in Figure 3c (solid lines). Both the electrostatic forces and excluded-volume effects contribute to formation of such structures.

It is also of interest to discuss the blocking correlation functions; the HNC approximation permits us to obtain insights into the "transmission" of the correlations between ions via the matrix subsystem. The blocking correlation functions as a function of electrolyte concentration are presented in Figure 3d. We observe that the behavior of $g_{ij}^{bl}(r)$ at larger distances is qualitatively similar to that observed for uncharged fluids in uncharged matrices, discussed in more detail in ref 31. However, there is an essential difference in the behavior of these functions for small distances. The blocking function, corresponding to equally charged ions, assumes high values at $r = 0$, similarly to hard spheres in hard-sphere matrices. On the other hand, the attraction between oppositely charged ions decreases the corresponding blocking function at small distances. The difference in the blocking functions between the equally charged and oppositely charged species increases with increasing electrolyte concentration. Therefore, one cannot claim that for a concentrated ionic fluid, confined in dense matrix (for which presumably the excluded-volume effects dominate), the electrostatic contribution to the blocking functions is of decreasing importance, at least not for small separations. We are not able, at present, to confirm these predictions by Monte Carlo results. Simulation of the blocking distribution function requires a sophisticated procedure, even for a simpler system consisting of a hard-sphere fluid in a hard-sphere matrix.[31]

Next we focus on the structural behavior of a 3−1 (model for $LaCl_3$) electrolyte solution. The cation in this system is slightly larger than in the $CaCl_2$ model solution, $\sigma_{Ca} = 7.03$ Å versus $\sigma_{La} = 7.75$ Å, so the excluded-volume effect is assumed to be similar in both systems. However, higher asymmetry in charge between the cation and anion may alter the structure of the confined electrolyte. The results for the 3−1 model solution are shown in Figures 4−6. These figures also contain the computer simulation results. The maximum concentration at which we obtained the ROZ result is 1.0 mol/dm^3. To obtain a convergent result at even higher concentrations would require prohibitively long runs. Theoretical predictions for the pdf of equally charged ions (Figure 4) agree with the trends obtained for 2−1 and 1−1 model electrolytes. We again observe a tendency for "pairing" of like-charge ions; the important changes in structure seem to occur in the range of concentrations between 0.001 and 0.1 mol/dm^3. In contrast to this behavior, there is no qualitative change of the unlike pdf, $g_{+-}(r)$, in the concentration

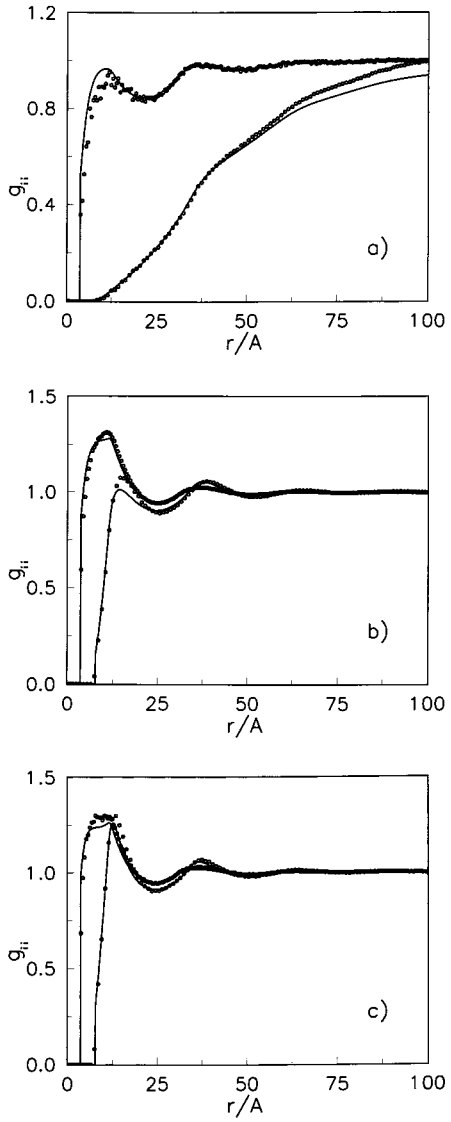

Figure 4. Like-charged (+ + and − −) pdf's for a model $LaCl_3$ solution. The electrolyte concentrations are (a) 0.001, (b) 0.1, and (c) 0.5 mol/dm^3. The lines and symbols denote the ROZ results and Monte Carlo data, respectively.

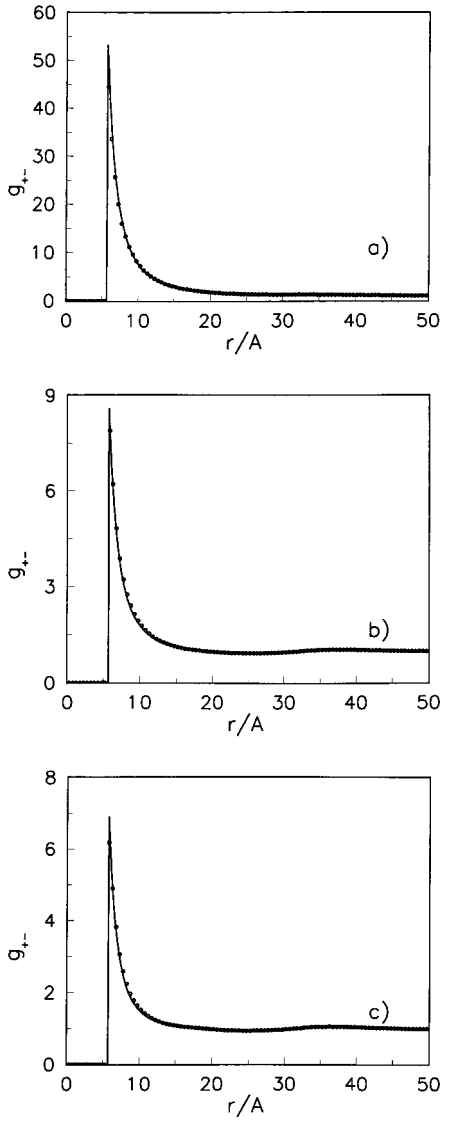

Figure 5. Distribution functions of a + − pair in a model $LaCl_3$ solution. Electrolyte concentrations and notation as for Figure 4.

range between 0.1 and 0.5 mol/dm^3 (we performed more calculations than are presented in Figure 5). It is important to mention that the theory agrees quite well with the computer simulation results over the entire concentration range studied here. The Monte Carlo results are presented in Figures 4−6 by symbols. The ROZ/HNC theory adequately describes the structural properties of confined 3−1 electrolytes; it is reasonable to expect that the theory would also perform quite well for less demanding cases, i.e., for 1−1 and 2−1 electrolyte solutions.

We proceed now to the last example, i.e., to the most highly asymmetric electrolyte studied in this work. We were interested in the structural changes caused by the hard-sphere confinement to a model 4−1 electrolyte mimicking $ThCl_4$ solution. The concentration range starting from 0.001 mol/dm^3 (dotted line) up to 0.275 mol/dm^3 (solid line) was explored, and the results are shown in Figure 7a,b. The model cation in this system is more than 3 times larger than the anion, while at the same time the charge asymmetry is 4−1. The larger diameter of the cation decreases the relative importance of electrostatic effects. The mutual repulsion between cations at low concentration alters in such a way that at 0.275 mol/dm^3 we have a high probability of finding two like-charged ions in contact (Figure 7a). Then, at slightly larger distances a maximum in $g_{ii}(r)$ shows the presence of triplets. At "high" (under this circumstances) ionic concentration, i.e., at 0.275 mol/dm^3, the ions are distributed close to each other, forming clusters. The layered structure of ions on the surface of a matrix particle can be easily seen from the shape of the ion−matrix pdf's, Figure 7c. At the end, we wish to comment on the blocking distribution functions for this case. Examples of these functions for (− −) and (+ −) pairs of ions are shown in parts d and e, respectively, of Figure 7. The magnitude of the $g_{ii}^{bl}(r)$ function at distances near zero increases with the increasing concentration of ions, while at the same time, the function goes to zero faster at larger distances (Figure 7d). On the other hand, the $g_{+-}^{bl}(r)$ function decreases in magnitude at small distances with increasing concentration, but it becomes slightly more structured for larger distances.

In Figure 8 we present a comparison of the pair distribution functions for a regular mixture (dashed lines) consisting of matrix particles and of the 3−1 ($LaCl_3$) electrolyte, with the pdf's for a corresponding partly quenched system (symbols). The pair distribution functions for bulk 3−1 electrolyte (in the absence of matrix species) are shown in the same figure by solid lines. In regular mixtures, where the "matrix" particles are allowed to equilibrate under the influence of ions present in

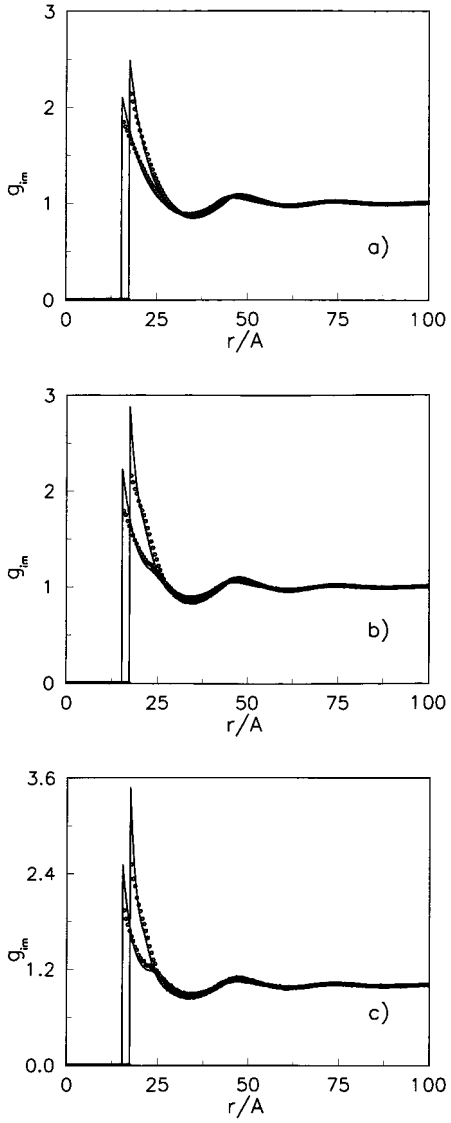

Figure 6. Ion−matrix pdf's for a model $LaCl_3$ solution; parameters and notation as for Figures 4 and 5.

the system, all the participating species are treated on an equal basis. Under this condition the usual OZ/HNC theory for mixtures applies. The concentration of electrolyte was 0.05 mol/dm^3 for all cases presented in Figure 8. The pair distribution functions for equally charged species are shown in Figure 8a. For bulk (pure) electrolyte solution, where there are no obstacles that mediate correlations, a stronger repulsion between cations compared to that between anions is evident. For a mixture considered at the same electrolyte concentration, we note a substantial probability of finding monovalent anions close to each other. According to the $--$ pair distribution function, there is a high probability for $-+-$ clusters. This behavior is much less pronounced for trivalent cations. Similar general behavior of the pair distribution functions can be seen for partly quenched systems under the same conditions. More precisely, the shape of the pdf for anions in the mixture is similar to that in the partly quenched system. The effective attraction between the cations is weaker in the partly quenched model compared to that in the mixture. A similarity in correlations of particles in partly quenched systems and in regular mixtures can also be observed for oppositely charged ions (Figure 8b). The aforementioned comparison illustrates structural similarities and disimilarities in the three cases. In conclusion we wish to mention that a rigidly fixed matrix produces a less pronounced structuring of like-charged ions than fully mobile obstacles of the same size.

Thermodynamic Properties. In addition to the pair distribution functions presented above, the thermodynamic properties of electrolyte solutions confined by the matrix were calculated. The excess internal energy per particle is given by[6,22]

$$\beta E^{ex}/N^1 = \frac{1}{2}\sum_{i=+,-}\sum_{j=+,-} x_i^1 \rho_j^1 \int \mathrm{d}\mathbf{r}\, g_{ij}^{11}(r)\, U_{ij}^{11}(r) \quad (11)$$

The isothermal compressibility $[\partial\rho_1/\partial(\beta P)]_T$, was calculated according to the well established compressibility equation[9−11,16,22,23]

$$\beta\left(\frac{\partial P}{\partial \rho^1}\right) = 1 - \rho^1 \sum_{i=+,-}\sum_{j=+,-} x_i^1 x_j^1 \int \mathrm{d}\mathbf{r}\, [c_{(s)ij}^{11}(r) - c_{(s)ij}^{12}(r)] \quad (12)$$

where ρ^1 is the total number concentration of ions. The general expressions given above are well-known, and these two properties are easy to calculate. This is not the case for the excess chemical potential, perhaps the most representative thermodynamic property of electrolyte solutions. For bulk electrolytes there are several ways of calculating the individual activity coefficient γ_i. One route, valid within the hypernetted-chain approximation, has been used on several occasions.[24,25] We have re-derived this expression (eq 10 of ref 24) within the replica formalism to read

$$\ln \gamma_i = -\rho^0 \mathbf{c}_{(s)i0}^{10}(\mathbf{0}) - \sum_{j=+,-} \rho_j^1 [\mathbf{c}_{(s)ij}^{11}(\mathbf{0}) - \mathbf{c}_{(s)ij}^{12}(\mathbf{0})] + 0.5\rho^0 \int \mathrm{d}\mathbf{r}\, h_{i0}^{10}(h_{i0}^{10} - c_{i0}^{10}) + 0.5 \sum_{j=+,-} \rho_j^1 \int \mathrm{d}\mathbf{r}\, [h_{ij}^{11}(h_{ij}^{11} - c_{ij}^{11}) - h_{ij}^{12}(h_{ij}^{12} - c_{ij}^{12})] \quad (13)$$

where $\mathbf{c}_{(s)}(\mathbf{0})$ denotes the Fourier transform of the short-range part of the direct correlation function at $k = 0$.

Changes in the structure of solution, brought about by the presence of the matrix, are reflected in the thermodynamic properties. These results are shown in Figure 9 and in Table 1. In Figure 9a we present results for the excess internal energy as a function of concentration for various model electrolytes. These results are qualitatively similar to the results for the corresponding bulk electrolytes. The presence of matrix particles makes the excess internal energy per ion more negative than it is for the corresponding bulk solutions (see also Table 1).

The concentration dependence of the compressibility of adsorbed electrolyte, shown in Figure 9b, exhibits nonmonotonous behavior. The electrostatic forces yield to increased compressibility in the low and intermediate concentration region, while at higher concentration the compressibility decreases; the behavior is qualitatively similar to that of a hard-sphere fluid in a hard-sphere matrix. Similar theoretical trends were observed for bulk 1−1 and 2−2 electrolytes.[32] The charge and size of the ionic species composing the electrolyte has a substantial influence on this property. For 1−1 electrolytes (NaCl and LiCl), these results are presented in Figure 9b by the solid and dashed lines; the compressibility is a decreasing function of electrolyte concentration. We observe a quite different behavior of the compressibility in the case of $LaCl_3$ and $ThCl_4$ solutions. In these cases the electrostatic attraction is strong enough to produce an increase in compressibility at low concentrations of the adsorbed fluid.

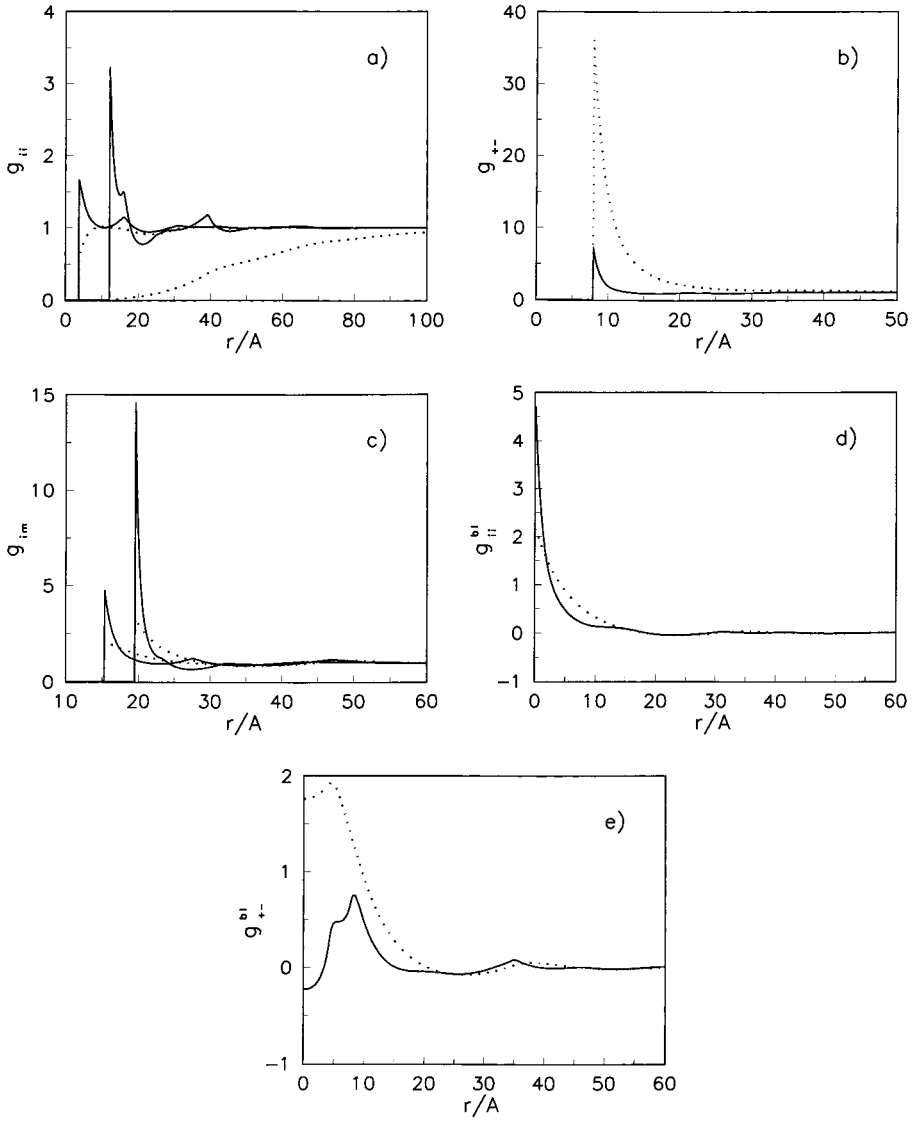

Figure 7. Pair distribution functions for (a) like-charged ions, (b) oppositely charged ions, and (c) ion−matrix pdf's for a model $ThCl_4$ solution at concentrations of 0.001mol/dm^3 (dotted line) and 0.275 mol/dm^3 solid line. Parts d and e show the blocking pdf's for − − and + − pairs, respectively.

The dominant role of electrostatic forces at low electrolyte concentrations can also be observed in Figure 9c. The concentration dependence of the mean activity coefficient is qualitatively similar to that obtained for bulk electrolytes. However, by comparing different curves in this figure one can easily see that the size ratio between the cations and anions plays an important role in determining the dependence of ln γ_{+-} on concentration. The curves for two different 1−1 electrolytes differ between themselves due to the larger diameter of the Li ion compared to the Na ion. On the other hand, the effect of charge asymmetry is clearly seen from our results for 2−1 and 3−1 electrolyte solutions. Ca ions (2−1 electrolyte) and La ions (3−1 electrolyte) have diameters which are close to each other, so the differences observed for these electrolytes are due to the difference in the charge of the cations. A higher charge of the cation in a salt yields a lower minimum for the mean activity coefficient.

A comparison of thermodynamic properties obtained by the ROZ theory and our Monte Carlo simulations for $LaCl_3$ model solution is given in Table 1. The results for pure electrolyte solutions obtained by the OZ/HNC theory (see, for example, ref 32) are given in parentheses. In general, the theoretical results for the excess internal energy and the mean activity coefficient agree reasonably well with the computer simulations. This limited comparison suggests that eq 13, in connection with the ROZ/HNC theory, could be quite useful in predicting the excess chemical potential for adsorbed electrolyte solutions. In addition, in Table 1 we present results for the excess internal energy per particle for a regular mixture of matrix and electrolyte ions. These results were obtained from the multicomponent OZ/HNC theory. The differences between the results for the two systems are small up to the intermediate concentrations studied here. However, great care must be exercised in describing the properties of a partly quenched model employing the results for a regular mixture. The latter results may merely serve as a helpful estimate and nothing more.

5. Concluding Remarks

Adsorption of electrolyte solution in a disordered hard-sphere matrix was studied by the ROZ/HNC and Monte Carlo methods. Five different electrolytes, described within the primitive model approximation, were studied in a broad concentration range. The matrix density and the diameter of matrix species were chosen according to the model of Kaminsky and Monson mimicking silica xerogel. This dense matrix provides a strong confinement

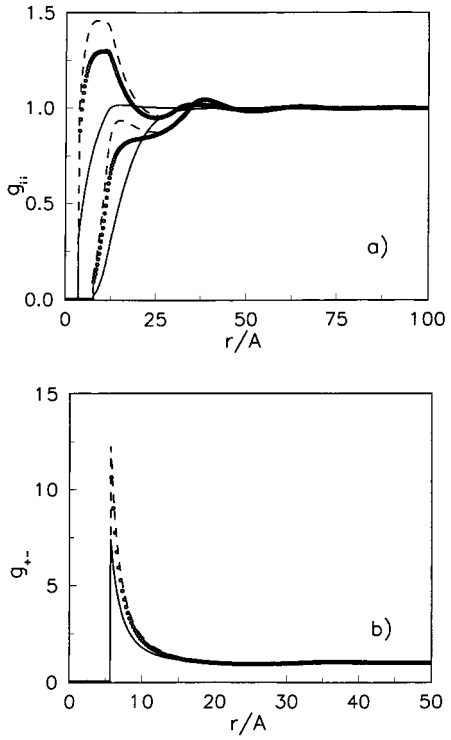

Figure 8. (a) Like-charged and (b) unlike-charged pdf's for $LaCl_3$ solution at 0.05 mol/dm^3 for three different calculations. The symbols pertain to the ROZ/HNC results for a partly quenched system. The results of the OZ/HNC theory for bulk electrolytes (solid lines) and for a regular mixture of "matrix" hard spheres and ions ($c_0 = 0.06$ mol/dm^3 (dashed lines)) are given for the sake of comparison.

for electrolyte solutions. Thermodynamic properties were calculated using well-known expressions for the internal energy and compressibility. The replica-type extension of the expression for the mean activity coefficient in the hypernetted-chain approximation was proposed and to a limited extent tested against the canonical Monte Carlo results. Reasonably good agreement of the ROZ/HNC theory and computer simulations for the structural and thermodynamic properties of a 3−1 electrolyte in the hard-sphere matrix was obtained.

The results presented above indicate the strong influence of a dense electroneutral matrix on the pair distribution functions and thermodynamics of confined electrolytes. It was observed that the range of correlations between ions drastically decreases with increasing electrolyte concentration. One important consequence of the presence of matrix particles is the onset of an attractive contribution to the potential of mean force between like-charged ions at small distances. This effect, shown most clearly in Figures 2a and 3a, can be explained via entropic arguments.[33] In general, the electrostatic effects are dominant at low concentrations, whereas the excluded-volume effects are of major importance in concentrated solutions of the adsorbed electrolyte. However, the calculations also show that electrostatic forces influence the blocking distribution functions even at high concentrations of adsorbed electrolyte.

A comparison of the results for the partly quenched systems at hand with the results for common mixtures consisting of matrix species and of an electrolyte shows certain similarities between the two systems. It seems that results for mixtures can serve as rough estimates of the properties of adsorbed electrolytes, at least for models in which matrix particles are larger than the ions and/or for dense matrices. A similar qualitative conclusion has been arrived at for uncharged systems.[6]

The results presented above suggest that properties of

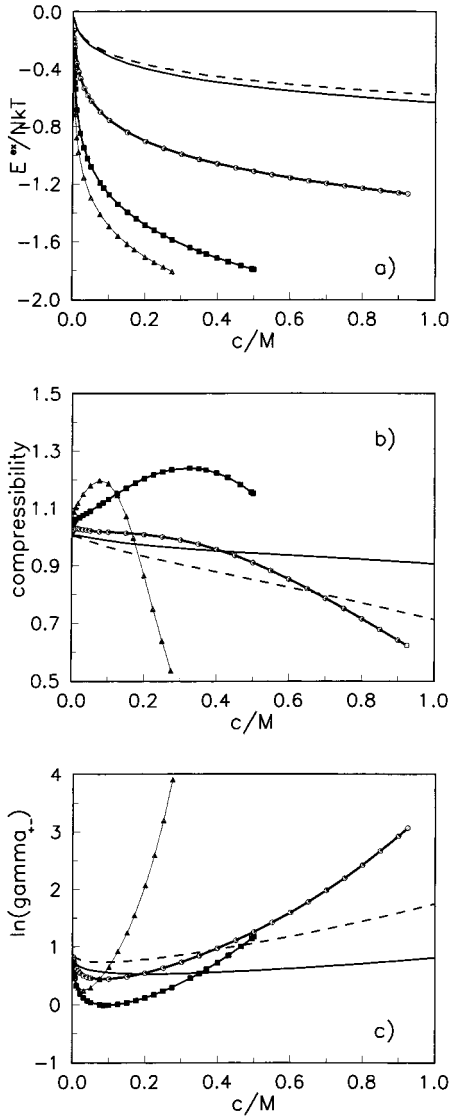

Figure 9. Thermodynamic properties of confined electrolytes from the ROZ/HNC theory: (a) excess internal energy per ion, (b) isothermal compressibility, and (c) mean activity coefficient. The solid line is for a model NaCl solution, and the dashed line is for a LiCl solution. The solid lines with symbols are for $CaCl_2$ (circles), $LaCl_3$ (squares), and $ThCl_4$ (triangles) model solutions.

TABLE 1: Reduced Excess Internal Energy Per Ion, $-E^{ex}/N^1k_BT$, and Mean Activity Coefficient, γ_{+-}, for a $LaCl_3$ Model Electrolyte in a Neutral Matrix as Predicted by ROZ/HNC Theory and Monte Carlo Computer Simulation[a]

	$-E^{ex}/N^1k_BT$			$\ln \gamma_{+-}$		
c_1 (M)	ROZ/HNC	MC	OZ/HNC	ROZ/HNC	MC	OZ/HNC
0.001	0.275	0.274 ± 0.002	0.276 (0.246)	0.687	0.68 ± 0.03	0.685 (−0.233)
0.01	0.688	0.697 ± 0.001	0.692 (0.615)	0.320	0.35 ± 0.02	0.310 (−0.574)
0.1	1.277	1.306 ± 0.001	− (1.183)	−0.0113	−0.06 ± 0.1	− (−1.043)
0.2	1.485	1.41 ± 0.01	− (1.382)	0.115	0.02 ± 0.1	− (−1.119)

[a] The results for a regular mixture of matrix and electrolyte particles obtained by the OZ/HNC theory are given for comparison. The excess energies for the corresponding bulk electrolytes are given in parentheses.

electrolyte solutions adsorbed in an uncharged confinement can, to a reasonable degree of accuracy, be predicted by the ROZ/

HNC theory. However, one cannot expect that a description of the ionic liquid−ionic vapor transition may follow from the latter theory. The liquid−vapor transition represents a challenging theoretical problem; the results following from this work may only serve as helpful insights for future developments. Nevertheless, we see a promising extension of the present research in application of the associative replica OZ equations[34,35] to ionic fluids via Wertheim's OZ integral equations for charged fluids.[36] Using the latter approach, a description of the behavior of electrolyte solutions in, for example, polyelectrolyte gels is within reach.

Acknowledgment. This work was supported in part by DGAPA of the National University of Mexico (UNAM) under Grant IN111597 and CONACyT of Mexico under Grant 25301-E. B.H. and V.V. acknowledge the support of the Ministry of Science and Technology of the Republic of Slovenia.

References and Notes

(1) *Fundamentals of Inhomogeneous Fluids*; Henderson, D., Ed.; Marcel Dekker: New York, 1992.
(2) Schoen, M. *Computer Simulation of Condensed Phases in Complex Geometries*; Springer-Verlag: Berlin, Heidelberg, 1993.
(3) Pizio, O. Adsorption in Random Porous Media. In *Computational Methods in Surface and Colloid Science*; Borowko, M., Ed.; Marcel Dekker: New York, 2000.
(4) Vlachy, V. *Annu. Rev. Phys. Chem.* **1999**, *50*, 145.
(5) Kaminsky, R. D.; Monson, P. A. *J. Chem. Phys.* **1991**, *95*, 2936.
(6) Vega, C.; Kaminsky, R. D.; Monson, P. A. *J. Chem. Phys.* **1993**, *99*, 3003.
(7) Bratko, D.; Chakraborty, A. K. *J. Chem. Phys.* **1995**, *104*, 7700.
(8) Madden, W. G.; Glandt, E. D. *J. Stat. Phys.* **1988**, *51*, 537.
(9) Given, J. A.; Stell, G. *Physica A* **1994**, *209*, 495.
(10) Given, J. A.; Stell, G. *J. Chem. Phys.* **1992**, *97*, 4573.
(11) Given, J. A.; Stell, G. In *XVI International Workshop on Condensed Matter Theories, San Juan, Puerto Rico, 1992*; Plenum: New York, 1993.
(12) Rosinberg, M. L.; Tarjus, G.; Stell, G. *J. Chem. Phys.* **1994**, *100*, 5172.
(13) Kierlik, P.; Rosinberg, M. L.; Tarjus, G.; Monson, A. *J. Chem. Phys.* **1997**, *106*, 264.
(14) Ford, D. M.; Glandt, E. D. *J. Chem. Phys.* **1994**, *100*, 2391.
(15) Pizio, O.; Sokolowski, S. *J. Phys. Stud.* **1998**, *2*, 296.
(16) Given, J. A. *J. Chem. Phys.* **1995**, *102*, 2934.
(17) Bratko, D.; Chakraborty, A. K. *Phys. Rev. E* **1995**, *51*, 5805.
(18) Chakraborty, A. K.; Bratko, D.; Chandler, D. *J. Chem. Phys.* **1994**, *100*, 1528.
(19) Deem, M. W.; Chandler, D. *J. Stat. Phys.* **1994**, *76*, 907.
(20) Muthukumar, M. *J. Chem. Phys.* **1989**, *90*, 4594.
(21) Hribar, B.; Pizio, O.; Trokhymchuk, A.; Vlachy, V. *J. Chem. Phys.* **1997**, *107*, 6335.
(22) Hribar, B.; Pizio, O.; Trokhymchuk, A.; Vlachy, V. *J. Chem. Phys.* **1998**, *109*, 2480.
(23) Hribar, B.; Vlachy, V.; Pizio, O.; Trokhymchuk, A.; *J. Phys. Chem. B* **1999**, *103*, 5361.
(24) Belloni, L. *Chem. Phys.* **1985**, *99*, 43.
(25) Belloni, L. *J. Chem. Phys.* **1988**, *88*, 5143.
(26) Lomba, E.; Given, J.; Stell, G.; Weis, J. J.; Levesque, D. *Phys. Rev. E* **1993**, *48*, 233.
(27) Simonin, J. P.; Bernard, O.; Blum, L. *J. Phys. Chem.* **1998**, *102*, 4411.
(28) Allen, M. P.; Tildesley, D. J. *Computer Simulations of Liquids*; Oxford University: New York, 1989.
(29) Wu, D.; Hui, K.; Chandler, D. *J. Chem. Phys.* **1992**, *96*, 835.
(30) Svensson, B. R.; Woodward, C. E. *Mol. Phys.* **1988**, *64*, 247.
(31) Meroni, A.; Levesque, D.; Weis, J. J. *J. Chem. Phys.* **1996**, *105*, 1101.
(32) Vlachy, V.; Ichiye, T.; Haymet, A. D. J. *J. Am. Chem. Soc.* **1991**, *113*, 1077.
(33) Asakura, S.; Oosawa, F. *J. Polym. Sci.* **1958**, *33*, 183.
(34) Trokhymchuk, A.; Pizio, O.; Holovko, M. *J. Phys. Chem.* **1996**, *100*, 17004.
(35) Trokhymchuk, A.; Pizio, O.; Holovko, M. *J. Chem. Phys.* **1997**, *106*, 200.
(36) Kalyuzhnyi, Yu. V.; Vlachy, V.; Holovko, M.; Stell, G. *J. Chem. Phys.* **1995**, *102*, 5770.